

Application of classical thermodynamic principles to the study of oceanic overturning circulation

By HERMAN G. GADE^{1*} and KARIN E. GUSTAFSSON^{2†}, ¹*Geophysical Institute, University of Bergen, Allegaten 71, N-5007 Bergen, Norway;* ²*Department of Oceanography, Earth Sciences Centre, Göteborg University, SE 405 30 Göteborg, Sweden*

(Manuscript received 24 March 2003; in final form 8 January 2004)

ABSTRACT

Stationary deep-reaching overturning circulation in the ocean is studied by means of classical thermodynamic methods employing closed cycles in pV -space (p , pressure; V , volume). From observed (or computed) density fields, the pV -method may be used to infer the power required for driving a circulation with a given mass flux, or, if the available power is known, the resulting mass flux of the circulation may be assessed. Here, the circulation is assumed to be driven by diapycnal mixing caused by internal disturbances of meteorological and tidal origin and from transfer of geothermal heat through the ocean bottom. The analysis is developed on the basis that potential energy produced by any of these mechanisms is available for driving a circulation of the water masses above its level of generation. The method also takes into account secondary generated potential energy resulting from turbulence developed by the ensuing circulation.

Models for different types of circulation are developed and applied to four types of hemispheric circulation with deep-water formation, convection and sinking in an idealized North Atlantic. Our calculations show that the energy input must exceed 15 J kg^{-1} for a cycle to the bottom to exist. An energy supply of 2 TW would in that case support a constant vertical mass flux of 3.2 G kg s^{-1} (3.1 Sv). Computed mass fluxes reaching the surface in the subtropics, corresponding to the same energy input, range between $2.3\text{--}5.2 \text{ G kg s}^{-1}$, depending on the type of convection/sinking involved. Much higher flux values ensue with ascending water masses reaching the surface at higher geographical latitudes.

The study reveals also that compressibility of sea water does not enhance the circulation. An incompressible system, operating within the same mass flux and temperature range, would require about 25% less energy supply, provided that the circulation comprises the same water masses. It is furthermore shown that the meridional distribution of surface salinity, with higher values in the tropics and lower values in regions of deep-water formation, actually enhances the circulation in comparison with one of a more uniform surface salinity. With a homohaline North Atlantic, operating within the same temperature range as presently observed, an increase of 66% of power supply would be required in order that the mass flux of the overturning circulation should remain the same.

1. Introduction

1.1. Historical and other relevant background

One of the earliest examples of recognition of basic conditions allowing deep-reaching circulation related to thermal convection from the sea surface is a contribution by Sandström (1908), referring to practical experiments with sea water in a tank. The essence of the observations was expressed in a simple statement that in order for sustained thermally induced circulation to exist, the heat source would have to be situated below the level of the heat sink (Sandström's theorem). In a paper from

1916 Sandström states that the actual variable here was pressure rather than depth, as a consequence of the Carnot cycle and the Bjerknes circulation theorem (Bjerknes 1898). The basic principles of the process have later on been adequately explained by Defant (1961), who also presented graphs of Carnot cycles to support the description. It was acknowledged that according to the theory, thermally induced meridional circulation based on the surface radiation and heat exchange necessarily would be limited to a fairly thin upper layer of the ocean. The validity of the theory had meanwhile been questioned by Jeffreys (1925), who argued that lateral density difference necessarily would induce circulation. It is however questionable whether the arguments of Jeffreys are valid without mixing being included as a necessary part of the process, which he actually did in his equations.

The existence of a substantial meridional deep convective type circulation has long been recognized as a fact, yet according to

[†]Present address: National Environmental Research Institute, DK-4000 Roskilde, Denmark.

*Corresponding author.
e-mail: herman.gade@gfi.uib.no

Huang (1999) it has for many years posed as a puzzle in the light of Sandström's theorem. This is evident from a number of contributions to the literature, e.g. Proudman (1953), Godske et al. (1957), Defant (1961) and Colin de Verdière (1993). Other scientists, such as Munk (1966), Welander (1968), Sjöberg and Stigebrandt (1992) and Huang (1999) among others, have recognized overturning ocean circulation as a direct consequence of diapycnal mixing as an active process taking place at all depths in stratified waters. As explicitly demonstrated in the papers of Sjöberg and Stigebrandt (1992) and Munk and Wunsch (1998), the energy required for maintaining such circulation depends, to a great extent, on conversion of ocean tides to internal tides and eventually to turbulence. This mechanism has strong similarity to convective-type exchanges in fjords that had been observed by Gade (1968) and Gade and Edwards (1980), and successfully explained by Stigebrandt (1976, 1979) as a result of turbulence generated by tidal-induced internal waves.

Further support of the role of eddy diffusion as a major mechanism for driving overturning circulation in the ocean was provided by Huang (1999). He developed theoretical solutions to steady density driven circulation within a loop enclosed in a tube, resulting from a heat source and a heat sink placed at diametrically opposite points of the loop. Heat was then subject to conduction (constant conductivity) from the source toward the sink. The experiments of interest in this connection were those in which the heat source was located at levels above the sink, establishing locally stable stratifications. The solutions showed that circulation would indeed take place and with a strength practically linearly dependent on the coefficient of heat conduction. The experiment would thus give support to both Sandström's conclusion, where eddy conduction was not considered, and to the comments of Jeffreys (1925), who included eddy diffusion in his equations.

1.2. Objectives of the present study

We will show how closed circulation cells such as meridional overturning can be studied in terms of the classical thermodynamic method employing closed cycles in pV -space (p , pressure; V , volume). Although several authors (Sandström 1916; Proudman 1953; Defant 1961; Huang 1999) have mentioned the use of the pV -diagram as a means to study the energetics of the thermohaline circulation in the ocean, we have not been able to find examples of such use. It has therefore been a tempting task to examine if the method could be of practical use in oceanography.

The paper consists of five sections. In the following (Section 2) we present the major energy sources and estimates of their magnitudes. In Section 3 we analyze properties of idealized diffusive-advective circulations in a single-spaced hemispheric ocean basin and corresponding representations in the pV -space. The state variables are assumed to be laterally homogeneous, and so also are the processes leading to generation of potential energy. Models utilizing classical thermodynamic principles are

established for (1) convection/sinking to any (one) given pressure level, and (2) convection/sinking to any range of (or all) pressure levels in the ocean basin. All examples are based on cycles originating at the sea surface. Distinction is made between systems with sinking water reaching directly the level of neutral buoyancy and systems in which density transformation also takes place along an isobaric path until the intruding water is neutrally buoyant in the main water mass. In Section 4, the models are applied to three forms of assumed circulation cycles in an idealized North Atlantic, all based on observed properties of the (rising) main water mass in the system. A fourth example deals with continuously distributed cycles associated with the sinking of Norwegian Sea Deep Water (NSDW) into the North Atlantic. The purpose is to demonstrate how the pV -method may be used for determining values of the mass flux of overturning circulation, in the three first cases on a purely hypothetical basis, in the fourth oriented toward a real case. The determined mass (or volume) fluxes (transports) are surprisingly low in comparison with values met in the literature, a result that is attributed to the constraints of the model applications, of which the most important is that the ascending water masses are assumed to surface with properties typical of eastern areas of the subtropical gyre. The last section (Section 5) is a discussion of various aspects of the theory, its advantages and shortcomings. It is emphasized that the paper focuses on exploring the method and is not meant as a study of the North Atlantic. Comparison is made with the classical method of describing diapycnal mixing in terms of a turbulent diffusivity and inherent limitations. Moreover, the influence of compressibility of sea water and the surface distribution of salinity is evaluated on the basis of actual computations for comparable parameter ranges. At the end, we discuss the impact of potential energy generated from geothermal heat transfer.

2. Energy sources for large-scale thermohaline circulation

Sustained thermohaline circulation of the oceans is a manifestation of conversion of extensive potential energy to large-scale kinetic energy within the system. A substantial amount of this conversion comes as a consequence of elevation of the sea surface in regions of low geographical latitudes. The process requires a continuous production of potential energy. Production of potential energy in the water column is mainly the result of diapycnal mixing in the interior of the ocean and geothermal heat transfer through the ocean floor. To some extent, the production of potential energy is directly influenced by the meridional distribution of precipitation and evaporation. Brief accounts of these processes are given below.

2.1. Generation of potential energy by diapycnal mixing

Turbulent diffusion is a form of mixing in which mass is exchanged principally without loss or gain of volume. However, wherever the state variables undergo changes, so also will the

specific volume, obeying the equation of state. A typical example is the warming of cold bottom water by mixing with warmer water above. Becoming thus gradually warmer, the bottom water will be less compressible and expand more than the corresponding contraction of the warmer water from above. Thus, under such circumstances a given volume may increase wherever the thermobaric effect is stronger than the normal isobaric volume contraction of mixing.

As a process, turbulence requires a considerable amount of energy to be supplied in order for it to develop and exist, even for a relatively small or limited period of time. With respect to turbulent diffusion of matter in stably stratified waters, it has for some time been recognized that only a minor proportion of the energy going into turbulence is available for doing work against gravity, i.e. contributing to increasing the potential energy of the water column. This proportion, referred to as the flux Richardson number (R_f), is of the order of 1/10. Here, the value 0.15 will be used following the suggestion by Osborn (1980), but values as low as 0.05 have been reported (Stigebrandt 1979; Pedersen 1980; Arneborg 2002).

The efficiency of introduced energy to produce work against gravity has long been the subject of debate. Reference is made to R_f and to the related 'efficiency' $\gamma = R_f/(1 - R_f)$ pertaining to the ratio of produced potential energy to the total dissipation of initial and secondary and subsequent manifestations of induced kinetic forms developed within the same ocean.¹ Several authors make use of an empirical value of $\gamma = 0.176$ (or 0.18) from $R_f = 0.15$.

About one third or 0.7 TW of the total M2-dissipation occurs in the open ocean (Egbert and Ray 2000, 2001; Gustafsson 2001). Extrapolating the result to all tidal components, Egbert and Ray (2000, 2001) suggest a total of about 1 TW of open ocean tidal dissipation. The energy flux from penetration of wind generated disturbances has been estimated to be about 1 TW (Wunsch, 1998; see however Wunsch and Ferrari, 2004, for a recent discussion of this estimate). Using these estimates, the combined energies available for diapycnal mixing in the deep ocean would come to about 5.43 mW m^{-2} . With $R_f = 0.15$ this gives a global average figure for production of potential energy due to diapycnal mixing of about 1.0 mW m^{-2} .

This generation of potential energy by diapycnal mixing in the ocean has traditionally been dealt with in the literature by use of an eddy coefficient K_z (Munk 1966; Munk and Wunsch 1998). In order to facilitate comparison with the present method employing the $p\alpha$ -cycle a simplified example of the K_z method is

presented in Appendix A. It is shown that for a stationary system the net energy required by diapycnal mixing in a Boussinesq fluid to bring a unit mass of water up through the water column from level $-D$ to the surface is

$$I = g \int_{-D}^0 \frac{\rho_{-D} - \rho(z)}{\rho_{-D}} dz. \quad (1)$$

Here ρ_{-D} and $\rho(z)$ are the potential densities of the bottom water and ambient water, respectively. With a non-Boussinesq fluid, the volume flux grows up through the water column, in which eq. (1) gives a much too high value. However, the corresponding non-Boussinesq form of eq. (1) allows it to be reduced to eq. (1) if pressure were the only factor affecting the volume of a particle and ρ_{-D} is replaced by the potential density of the bottom water at level z . Taking the effect of normal (isobaric) volume contraction under vertical mixing into account, the mentioned form will not be exact but will give a slight underestimate, although in many cases an adequate measure of the net work involved.

2.2. Geothermal heating

Whereas eddy diffusion of heat from above, or the corresponding upward eddy diffusion of mass, is the least effective way the ocean can function as a heat engine, geothermal heat conducted through the ocean floor is readily available and contributes to the production of potential energy of the water column. Heat transferred through the bottom of the ocean causes a slight increase of temperature of the bottom water. Although thermal convection may take place within a bottom layer of limited thickness, signs of extended convection are rarely observed except over particular hot spots along submarine ridges and volcanoes. This feature may be linked to renewal by advection from other regions and to vertical exchange with lighter water from above. Nevertheless, the increase in temperature affects the density of the lower part of the water column and thereby enhances vertical mixing generated by other mechanisms.

Apart from the mentioned effects of a slight increase of temperature, the immediate effect of geothermal heat transfer is thermal expansion, and because this takes place under pressure, work is performed and instantly converted to potential energy in the water column. If the stratification remains everywhere stable, the generation rate of potential energy is at its maximum. This may be computed per unit surface from

$$\phi_{GH} = g\bar{\rho}D \frac{\alpha \dot{Q}}{\rho_{BCp}}. \quad (2)$$

Here, D is the depth of the water, $\bar{\rho}D$ is the total mass per unit surface of the water column, α is the coefficient of thermal expansion, \dot{Q} is the heat transfer rate (density) and ρ_{BCp} is the heat capacity per unit volume of the bottom water. A development involving the heating of a thin bottom layer, leading to eq. (2) is presented in Appendix B. It is shown that the production of potential energy is actually slightly less than given by eq. (2),

¹This result follows directly from the simplified turbulent energy equation and applies to the primary production of potential energy and related dissipation. The expression will also hold for initial and subsequent generations of potential energy in a stationary closed system provided that the conversion of secondary and subsequent kinetic forms is governed by the same R_f . The result is a manifestation of recirculation of energy.

depending on the thickness of the homogeneous bottom layer (eq. B4). Note that the expression (2) is independent of choice of reference level for the potential energy. Correspondingly, the total rate of initially generated potential energy ϕ_{GH} in any defined ocean system may be expressed by

$$\Phi_{GH} = \int_A \phi_{GH} dA \quad (3)$$

where A is the horizontal area of the corresponding ocean with stably stratified water masses. However, because of internal redistribution of mass all produced potential energy given by eq. (3) will not be available to support overturning ocean circulation (discussed in Section 5.6).

Geothermal heat flux densities through the ocean bottom have been estimated with a global average value of about 88 mW m^{-2} (Stein and Stein 1992). The general tendency is a distribution with higher values in more recent ridge structures, declining to a background value of 46 mW m^{-2} on the abyssal plains between 5000 and 6000 m depth. We have estimated the production of geothermally generated potential energy in the North Atlantic to 0.11 mW m^{-2} as an average. This is about 11% of the value (0.99 mW m^{-2}) resulting from diapycnal mixing generated by tidal and wind effects alone.

2.3. Generation of potential energy by precipitation/evaporation

For a steady-state system, any flux of mass at the free surface will represent a corresponding flux of potential energy. If this energy is to become available to the overturning circulation, the supply will have to take place at levels above those of subtraction. By and large, this is not the case in the world oceans as evaporation occurs mostly where the sea level is high, and precipitation where sea level is low.

Precipitation (/evaporation) is a flux of mass to (/from) the sea surface and consequently representing flux of potential energy. Any geopotential surface below the lowest level of the sea surface may be used as a reference level. By definition, the total flux of potential energy (out of the system) by evaporation/precipitation over a given surface of the ocean σ is

$$-\Phi_{ep} = \int_{\sigma} \rho_0 g (H + z) \mathbf{v} \cdot d\boldsymbol{\sigma}. \quad (4)$$

Here, ρ_0 is the freshwater density, H is the height of a reference point at the sea surface above the chosen reference level, \mathbf{v} is the rate of evaporation/precipitation and z is the level of the sea surface relative to the chosen reference point. For the world oceans as a whole, or any stationary closed ocean, the first part of the integral vanishes, so in that case the loss of potential energy is simply

$$-\Phi_{ep} = g \int_{\sigma} \rho_0 v_n z d\sigma \quad (5)$$

independently of the level of the reference point. The integral has the form of a covariance. For the oceans as a whole, the value of the integral is positive, implying a net loss of potential energy. Thus, the global distribution of evaporation and precipitation per se does not support the large-scale overturning circulation in the ocean.

The world oceans average loss of potential energy by evaporation/precipitation and runoff is less than 0.02 mW m^{-2} according to our estimates. This amounts to about 13% of the production of potential energy by geothermal heat transfer to the oceans.

3. Analysis of stationary single basin overturning circulation

In this section we present the pV -diagram and models for how it can be used to calculate the mass flux of a given circulation cell. The models may be applied to the meridional overturning or circulation cells of other systems such as that of the Mediterranean Sea or the Black Sea.

Consider a single basin system where the surface water undergoes continually property modifications that eventually lead to the sinking of water masses at high geographical latitudes. In a stationary system, some fraction of the sinking water will find its way to the deepest depression in the basin. The rest of the sinking water is likely to become distributed over a range of depths although certain depth ranges may be favored. The process involves intrusions, assimilations and displacements, of which the consequence is a continuous general uplift of the entire water column. The system of closed circulations is shown schematically in Fig. 1.

Assume now that the specific volume α in the main water mass is a continuous function of pressure only and that the properties of the sinking water coming to rest at a given level are known from observations. We shall, in the following, study the transformation of a unit mass of water as it progresses in a closed circulation cell such as described above. A suitable way of doing that is by means of the classical pV -diagram (hereafter denoted $p\alpha$ -diagram with reference to α as a symbol of specific volume in oceanography). It follows from the prescribed conditions that each of the shown

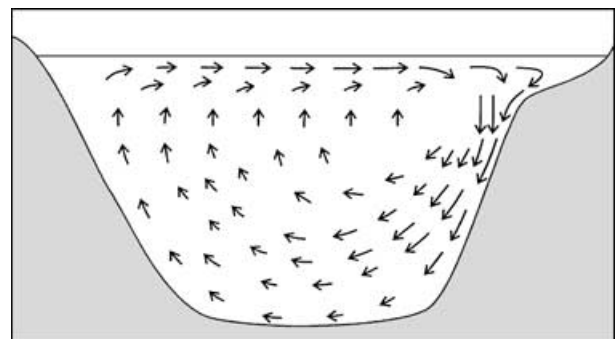


Fig 1. Schematic diagram of hemispheric single-basin meridional overturning circulation cells resulting from sinking with intrusions in a range of levels extending to the bottom.

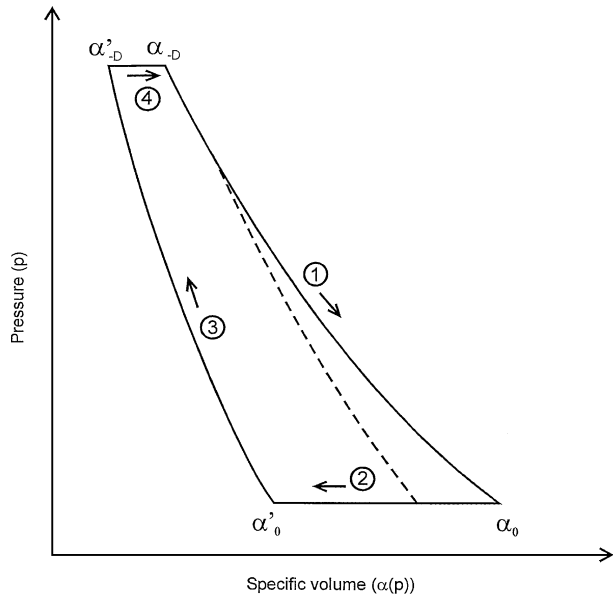


Fig 2. Schematic diagram of transformation cycle in the $p\alpha$ -space corresponding to circulation in a single cell as in Fig. 1. The dashed line is an example of adiabatic transformation path resulting from sinking of water of potential specific volume corresponding to the intersection point.

circulations has a corresponding $p\alpha$ -representation that is completely determined by the distribution of specific volume versus the pressure along the path. Figure 2 shows a schematic diagram of such a cycle corresponding to a circulation operating between two isobars.

3.1. The $p\alpha$ -cycle

Consider a unit mass of water participating in a cycle such as shown in Fig. 2. Here, path (1) is the gradual change of specific volume (α) due to vertical advection and diffusion and possibly some influence of geothermal heating, while the pressure (p) reduces during the ascent. The unit mass is then assumed to move along path (2) at constant surface pressure, while the specific volume changes from α_0 to α'_0 . From there the parcel descends along path (3) (specific volume, $\alpha'(p)$) until it has reached its deepest level, the corresponding specific volume being α'_{-D} . Translation along the isobaric path (4) closes the cycle. Through geothermal heating and vertical diffusion the specific volume increases during this transit until the end point α_{-D} is reached. A real version of such a diagram is that of Fig. 3 where meridional overturning in the North Atlantic is depicted. Because of the overwhelming influence of pressure on the specific volume, a more practical way to illustrate the process is to plot the isobaric difference of the specific volume $\Delta\alpha(p) = \alpha(p) - \alpha'(p)$ against pressure. An example of this is shown in Fig. 4 which shows the transformed cycle of Fig. 3.

The net amount of work performed against pressure (universe) by the circulation of a unit mass during one cycle is simply

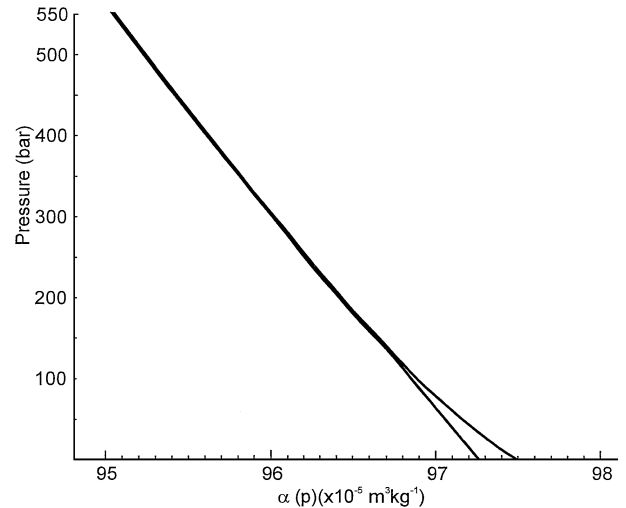


Fig 3. Actual $p\alpha$ -representation of circulation cell originating with NSDW assumed to reach the 550-bar level in the North American basin followed by uplift as observed water mass of mid- and low-latitude North Atlantic.

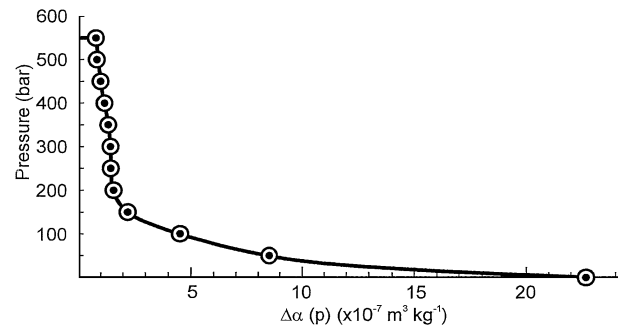


Fig 4. Transformation cycle of NSDW of Fig. 3 represented by $\Delta\alpha(p) = \alpha(p) - \alpha'(p)$ versus pressure.

$$J = \oint p \, d\alpha. \quad (6)$$

This work is measured by the area inside the closed curve. By suitable transformation of eq. (6) and expansion it may be shown that under hydrostatic conditions

$$J \approx g \int_{-D}^0 \frac{\rho_{-D} - \rho(z)}{\rho_{-D}} dz + g \int_{-D}^0 \frac{\rho'(z) - \rho_{-D}}{\rho_{-D}} dz \quad (7)$$

is an alternative (although approximate) representation of the work performed during one cycle. For details, see Appendix C. However, because of the non-Boussinesq nature of eq. (7), its interpretation is not as straightforward as it may seem. We may handle this situation by replacing ρ_{-D} in the numerators of both terms on the right-hand side (rhs) by its potential density at level z along path (1). In that case, the first rhs term will be nearly the same as that of eq. (1), actually slightly less, and a measure of the work against gravity in bringing a unit mass from level $-D$ to the surface. The second of the rhs terms will then be slightly positive, indicating that the mixing taking place within the sinking

water column and subsequent advection along path (4) actually performs a small amount of work against pressure. Whether referring to eq. (6) or eq. (7) the generated energy is initially in the form of potential energy, but is subsequently released as kinetic energy. A major part of this is lost to dissipation. The remaining minor part is recirculated by its contribution to diapycnal mixing and resulting potential energy. This means that the actual net power required from external sources to maintain the circulation is correspondingly less than implied by eq. (7) and also likely less than the first integral of eq. (7), or its equivalent K_z -form (A1) (simplified), applied to the upward branch only.

3.2. Mass flux and energy considerations

In this section a method is developed by which the mass flux in stationary large-scale overturning circulation in a single basin may be determined. The method requires knowledge of the density field of the main rising water mass and also of the power available for driving the circulation. On the basis that each contributing circulation path has a depth limitation $z(p_e)$, the corresponding $p\alpha$ -cycle is similarly limited by the lower level pressure p_e . With the specific volume of the sinking as well as that of the rising water known, it follows that an energy function $q(p_e)$ may be defined that is solely a function of the limiting pressure (p_e) of the particular cycle. Thus, with the possible circulations in nature sufficiently well established, the corresponding energy function $q(p_e)$ is in principle similarly known. The energy function may then be determined from the $p\Delta\alpha$ -diagram (as in Fig. 4) by

$$q(p_e) = \int_0^{p_e} [\alpha(p) - \alpha'(p)] dp = \int_0^{p_e} \Delta\alpha(p) dp. \quad (8)$$

From this it also follows that $\Delta\alpha = \partial q(p)/\partial p$. In addition to the function $q(p_e)$, a few other functions and expressions are useful. These will be defined in the following sections. In many of the following applications p_e will appear as a free independent variable. In these cases the index is superfluous and has been eliminated.

3.2.1. Mass fluxes. Let $m(p)$ denote the mass transport density² of the sinking water coming to rest at the pressure level p . A function $m(p)$ defined as

$$M(p) = \int_0^p m(p') dp' \quad (9)$$

will then be a measure of the total (cumulative) mass flux by the circulation cells acting between the surface down to any pressure $p' \leq p$. If extended to the deepest possible depth in the basin ($p = p_B$), the integral becomes

$$M_T = \int_0^{p_B} m(p) dp. \quad (10)$$

M_T comprises all overturning circulation in the basin and is a measure of the total (diffusive and advective) mass flux reaching the surface (or near surface levels) in the process.

At any pressure level p there is a slowly upward advective and diffusive mass flux $F(p)$ balancing the total of the descending water masses to the levels below. Formally this mass flux may be written

$$F(p) = \int_p^{p_B} m(p') dp'. \quad (11)$$

It follows that

$$m(p) = -\frac{\partial F(p)}{\partial p}. \quad (12)$$

3.2.2. Energy flux balances. We shall, in the following, assume that the effective³ value of the power supply, here specified as power supply density (per unit dimension of pressure change) in the basin, $\omega(p)$, is known. The corresponding total of power available above level p is consequently

$$\Omega(p) = \int_0^p \omega(p') dp'. \quad (13)$$

With the integration extending to the deepest level in the basin the integral is a measure of the total amount of power (Ω_T) available for producing work against gravity

$$\Omega_T = \int_0^{p_B} \omega(p) dp. \quad (14)$$

The power supply needed to fulfill the requirements of steady overturning circulation down to the pressure level p in the basin, with no sinking taking place to levels below p , is

$$W(p)_{\text{lim}} = \int_0^p m(p') q(p') dp'. \quad (15)$$

Here, $q(p')$ is the energy requirement per unit mass participating in the circulation to level p' and $m(p')$ is the corresponding mass flux density to this level. With sinking also taking place to levels below $p(z)$ the corresponding form can be shown to be

$$W(p) = \int_0^p m(p') q(p') dp' + F(p) q(p). \quad (16)$$

The last term above is the power required to deal with the mass flux $F(p)$ entering through the pressure surface p from below. The specific requirement (per unit mass) of the latter is identical to that of an intrusion at level p . If the integral of eq. (16) is extended to the deepest level, the last term vanishes in which case eq. (16) reduces to

$$W_T = \int_0^{p_B} m(p) q(p) dp. \quad (17)$$

In order for the process to exist it must adjust to the available power density (14). This condition follows from differentiation

²Transport density' $m(p)$ is here defined as transport per unit pressure difference (δp) in the sense that $m(p)\delta p$ is the rate of mass of sinking water coming to rest within a layer of thickness $\delta p/(\rho g)$ at pressure p .

³'Effective' is here used in the sense that an equivalent contribution to the production of potential energy in the water column takes place.

of eq. (16):

$$\omega(p) = \frac{dW(p)}{dp} = m(p)q(p) + \frac{\partial F(p)}{\partial p}q(p) + F(p)\frac{\partial q(p)}{\partial p}. \quad (18)$$

Taking into account eq. (12), the expression above reduces to

$$\omega(p) = F(p)\frac{\partial q(p)}{\partial p}. \quad (19)$$

In application of eq. (19) the gradient $\partial q(p)/\partial p$ is simply the isobaric difference $\Delta\alpha(p)$ (previously introduced in eq. 8) between the rising and the sinking water. In our study the mass flux $F(p)$ is the unknown quantity to be determined. This means that it becomes essential to assess the vertical distribution of the power density $\omega(p)$.

Although the total flux of energy available for mixing in the oceans has been estimated, it has not yet been convincingly demonstrated how this energy flux is distributed within the sea, specifically its distribution with depth. Nevertheless, in the next section we adopt a concept proposed by several referenced authors, linking the rate of energy conversion to the buoyancy frequency. This leaves us with determining $q(p)$, which may be determined from the $p\alpha$ -diagram, but actually depends on the particular form of convection and subsequent sinking taking place in the system. Facing this problem we have chosen to limit the computations to two extreme forms leading to limiting values for the vertical mass flux distribution $F(p)$.

3.3. Assessment of the vertical distribution of power toward diapycnal mixing

Although it seems to be fairly well documented to which degree energy from the barotropic tides in the world oceans is constantly being redistributed to internal modes, it is not at all obvious where, or at which levels, these energy forms convert to turbulence. In this paper we have chosen a simplest possible model, one in which the wave energy density and wind supplied power available for conversion are distributed vertically as a function of the buoyancy frequency N . The relevant terms of the simplified turbulent energy equation may then be written

$$\rho N^2 K_z(z) = \gamma C(z) \quad (20)$$

where $K_z(z)$ is the vertical eddy diffusivity and $C(z)$ is the energy conversion rate to turbulence per unit volume. On assumption that γ is the same for tidal and wind generated disturbances as well as from the ensuing circulation from these sources and geothermal heating, integration over the entire ocean basin leads to

$$\begin{aligned} \int_0^D \rho N^2 K_z A(z) dz &= \gamma \int_0^D C(z) A(z) dz \\ &= \gamma(E_{WT} + \Phi_{GH}) = \Omega_T. \end{aligned} \quad (21)$$

Here, $A(z)$ is the area of the horizontal cross-section, E_{WT} is the total power supply from wind and tidal action, and Φ_{GH} is the generation rate of potential energy by geothermal heat transfer

to the ocean basin (eq. 2); however, all limited to the part with an overall static stability.

A possible inverse effect of the static stability on vertical eddy fluxes has already been pointed out by Taylor (1931). Fjeldstad (1936) employed a similar relationship in assessing frictional effects in tidal currents. Since then, many have been tempted to apply relationships of the form

$$K_z = a(N^2)^{-\alpha} \quad (22)$$

in both experimental and theoretical approaches.⁴ From many experiments conducted in different waters, possible relationships of the form above have been discussed by various authors, but seemingly with different results. Gade reported in 1970 of extended experiments in the Oslofjord pointing toward an α in the range of 3/4 to 4/5 (Gade and Edwards 1980). Other experiments support the general form of relationship, but with different values of the exponent. Thus, Göransson and Svensson (1975) found $\alpha = 0.6$ for the Gothenburg Byfjord, and values as low as 0.5 have been reported by Stigebrandt and Aure (1989). This widespread dependency on α is possibly a consequence of internal convective adjustments in regions of lateral inhomogeneity.

Various authors have shown considerable interest in the matter from a more theoretical point of view. Among the earliest of these efforts to reach some conclusion on a purely theoretical basis was that of Welander (1968), who suggested α to be 1/2. Later contributions from Gargett (1984), Gargett and Holloway (1984) and Stigebrandt and Aure (1989) are partly in agreement with Welander's suggestion, but also leaving some doubt to the applicability of a form as simple as that.

In the present paper we have chosen to work with a relationship of the form (22) with $\alpha = 1/2$. With this value, substitution of eq. (22) into eq. (21) leads directly to

$$a \int_0^D \rho N A(z) dz = \gamma(E_{WT} + \Phi_{GH}). \quad (23)$$

By eq. (23) the factor (a) is determined. By changing to pressure units the corresponding power conversion rate (density) over the entire pressure surface is consequently

$$\omega(p) = a \frac{N(p)A(p)}{g}. \quad (24)$$

3.4. Total energy flux density toward meridional overturning circulation

In the previous sections we have dealt with the power supply to diapycnal mixing as the most important contribution to the energy budget of the hierarchy of cycles in the $p\alpha$ -space. A minor fraction of the potential energy generated from geothermal heating contributes to that effect through turbulence from the ensuing circulation. However, the major part of the power generated by

⁴The α introduced here has no relation to that of specific volume traditionally used in oceanography.

geothermal heating (adjusted for evaporation/precipitation) toward overturning circulation is released from the resulting pressure field. Because all circulation cells are assumed to reach down from the surface, we have applied the Sandström theorem implying that the potential energy generated by geothermal heating is available above the level of its generation.

3.5. Overturning circulation scenario 1: sinking to the deepest bottom only

With sinking to the bottom only, $F(p)$ becomes a constant $F = M_T$. Eq. (19) may then be integrated directly to yield

$$\int_{p_1}^{p_2} \omega(p) dp = F \int_{p_1}^{p_2} \frac{\partial q}{\partial p} dp = F \int_{q_{p1}}^{q_{p2}} dq = F(q_{p2} - q_{p1}) \quad (25)$$

where indices 1 and 2 refer to two arbitrary chosen pressure levels. For convection from the surface with sinking to the greatest depth, the left-hand side (lhs) of eq. (25) will be Ω_T , as of eq. (14), while the rhs, reducing to $M_T q(p_B)$, where $q(p_B)$ is the total area of the $p\alpha$ -cycle. The constant mass flux is then

$$M_T = \frac{\Omega_T}{q(p_B)}. \quad (26)$$

On the assumption that the total amount of available power (Ω_T) in the ocean basin is known, M_T is readily obtained from eq. (26) after $q(p_B)$ has been determined, most conveniently by numerical integration. This case is interesting because it tells how the power supply must be distributed vertically in order that the constant flux condition shall be satisfied. It is, however, practically impossible to find a data set which is virtually free from convection to any intermediate depth range. Determinations based on eq. (26) and eq. (19) applied to data from a real ocean basin will inevitably be affected and produce underestimates of the total mass flux at high levels and overestimates at low levels (high pressures).

3.5.1. Adiabatic convection/descent. As mentioned above, determination of the constant mass flux F according to eq. (26) depends on how $q(p_B)$, the energy requirement per unit mass participating in the cycle, is defined. With adiabatic convection/sinking (no mass or heat exchange during descent), the specific volume ($\alpha'(p)$) along path (3) will be that of an adiabatic, although this may not necessarily intersect with path (4) at the bottom. However, if it does, $\alpha'(p)$ may be determined through computation of the corresponding potential specific volumes up through the water column. Otherwise, as indicated in the schematic diagram of Fig. 4, the specific volume of the sinking water may differ from α_{-D} of the rising bottom water by an amount $\Delta\alpha(p_{-D})$, in which case the integration must be based on observed isobaric $\Delta\alpha(p)$ -values. An example of determination of M_T for the North Atlantic according to this concept is shown in Section 4.1.1.

3.5.2. Descent as observed bottom current down the continental slope. Wherever the deep-reaching sinking is known in

the form of a bottom current without appreciable intrusion, but with recognized entrainment, $F(p)$ will not remain a constant but be subject to a slight increase with p . In this case the specific volumes of both sinking and rising water will be affected in such a way that $\Delta\alpha(p)$ is reduced with a corresponding influence on $q(p)$ and $\partial q(p)/\partial p$. $F(p)$ may be derived from eq. (19) by substitution of the appropriate $\Delta\alpha(p)$ -values. However, in reality detrainment and intrusions are likely to occur and be revealed by reducing $F(p)$ -values with depth (as example of Section 4.2.2).

3.6. Overturning circulation scenario 2: sinking and intrusion to a range of depths

The basis for dealing with this scenario of single source convection and sinking to a range of depths is still eq. (19). In this case the main rising body of water is likely to be more strongly affected by the mixing with the sinking bottom current, a process that will show up by reduced isobaric difference values ($\Delta\alpha(p)$). In some cases the reduction may be so strong that $\Delta\alpha(p)$ virtually vanishes at great depths. As in Section 3.5.2 the relevant variables are $\Delta\alpha(p)$ and the power supply density $\omega(p)$ through thermal expansion and diapycnal mixing.

Up to now we have been concerned with convection and subsequent sinking of water deriving from one source, i.e. having an identifiable specific volume when leaving the free surface (or any other recognized pressure level). If, however, two or more sources contribute to the circulation, these may have different specific volumes and will then describe different sinking paths in the $p\alpha$ -space. Although the rising water may be assumed to be one laterally homogeneous body, each of the sources will be the origin of a particular $q_i(p)$ -function and with a corresponding $m_i(p)$ -function. The method such as developed in the previous sections will not handle this situation unless the ratios between the various $m_i(p)$ -values are given. These may be deduced by invoking other methods. However, the complexity of several sources contributing to the overturning circulation in a single ocean basin is outside the scope of this paper.

4. Application of selected models to conceptual forms of overturning circulation in the North Atlantic

4.1. Adiabatic sinking to the bottom in the North American Basin (scenario 1)

4.1.1. Adiabatic sinking of water having salinity and potential temperature of the bottom water itself. Although quite unrealistic it is here assumed that the water column in the mid- and low-latitude North Atlantic is the result of adiabatic convection and sinking to the greatest depths only. Subsequent diapycnal mixing and vertical advection followed by return toward high latitudes at near surface pressures close the circulation. In this, as in the following examples, the rising water (properties taken from Levitus and Boyer, 1994 and Levitus et al., 1994) is

assumed to reach the surface with properties similar to those found at the eastern outskirts of the subtropical warm water lens (25.5°N, 30.5°W), ($T = 22.946^\circ\text{C}$, $S = 37.295$). Whether the bottom water actually originates in the North Atlantic, or is a mixture of Antarctic Bottom Water (AABW), NSDW and North Atlantic Deep Water (NADW) is irrelevant, because the convecting water in this case is defined as one having the same salinity and potential temperature of the bottom water itself. For this purpose we have chosen the 550-bar level as our reference. This choice implies that the sinking water arrives at this level with a specific volume identical to that of the resident water. It is also a consequence of the specified circulation process that the net upward mass flux is constant, i.e. independent of depth.

With the circulation so defined the enclosed area of the corresponding $p\alpha$ -cycle is determined by integration of the isobaric difference between observed and computed *in situ* specific volumes (see Fig. 5) between $p = 0$ and $= 550$ bar. In this case the value of the integral is 15.48 J kg^{-1} , and this value is the least possible for any circulation reaching that depth. Under the adiabatic condition, the vertical mass flux ($F(p) = F$) must remain constant up through the water column. The value of $F(= M_T)$ follows by the use of eq. (26) after the available power has been assessed.

The total primary power input, and available for mixing in the North Atlantic south of the Greenland–Scotland ridge, is here established on the basis of computed $7.86 \times 10^{10} \text{ W}$ from the M2-tides for all water below 1000 m, and about $1.18 \times 10^{10} \text{ W}$ estimated for the levels above, excluding shelf waters, and then adjusted to include all tidal constituents (Egbert and Ray 2000), totaling $12.66 \times 10^{10} \text{ W}$. Deep-reaching wind effects are estimated on the basis of the overall global dissipation value of 2.8 mW m^{-2} given by Wunsch (1998). The corresponding total for the wind energy in the North Atlantic amounts to $11.7 \times 10^{10} \text{ W}$. Thus, the total energy flux to mixing in the interior from tidal and wind action adds up to $24.4 \times 10^{10} \text{ W}$. With an efficiency of 0.18 the production rate of potential energy by wind and tidal mixing comes to $4.39 \times 10^{10} \text{ W}$.

In addition to the potential energy resulting from the action of winds and tides, there is also a small contribution to diapycnal mixing resulting from geothermal heat transfer (eq. 23). Our computations based on eq. (2) with heat transfer data from Stein and Stein (1992) have given a value of $\Phi_{\text{GH}} = 0.47 \times 10^{10} \text{ W}$ for the North Atlantic. With the same efficiency as before, the corresponding contribution to potential energy by diapycnal mixing due to geothermal heating amounts to $0.09 \times 10^{10} \text{ W}$, giving a total of $4.48 \times 10^{10} \text{ W}$ generated by diapycnal mixing. With the potential energy related to geothermal heating included, a total of $4.96 \times 10^{10} \text{ W}$ is available to drive the circulation (see note at end of Section 5.6).

On the basis of the production rate of available potential energy and the computed 15.48 J kg^{-1} required for the specified cycle, the constant mass flux of the system comes to $3.20 \times 10^9 \text{ kg s}^{-1}$, equivalent to 3.12 Sv. The corresponding power den-

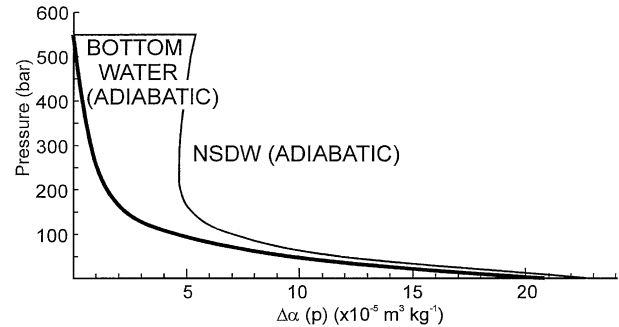


Fig 5. Hypothetical transformation cycle in the North Atlantic with adiabatic sinking of water having salinity and potential temperature of the bottom water at the 550-bar level and combined with specific volume of the main rising water mass as observed (heavy line). Also hypothetical cycle of adiabatic sinking of NSDW to the 550-bar level in the North Atlantic combined with rising water mass as observed (thin line).

sity requirement $\omega_0(p)$ for this mass flux is now obtained from eq. (19). The numerical values are listed in the second column of Table 1.

By integration of eq. (23) the corresponding coefficient (a) has been determined to $1.318 \times 10^{-7} \text{ J kg}^{-1}$. With that applied to eq. (24) the power conversion densities $\omega_1(p)$ deriving from diapycnal mixing have been obtained. To these values the contribution from the production rate of potential energy from geothermal heat has been added, and the total presented as $\omega_T(p)$.

As seen, there is a rough resemblance between $\omega_0(p)$ and $\omega_1(p)$. The latter of the two has clearly lower values in the upper

Table 1. Power requirements $\omega_0(p)$ to diapycnic mixing (in W Pa^{-1}) at selected pressure levels for computed hypothetical constant total vertical mass flux of $3.26 \times 10^9 \text{ kg s}^{-1}$, and distribution of power density to diapycnic mixing $\omega_1(p)$ according to eq. (27) ($\alpha = 1/2$), and $\omega_2(p)$ with $\alpha = 2/5$ in eq. (24). Columns 5 and 6 give estimated power density $\omega_\phi(p)$ to potential energy from geothermal heat, and $\omega_T(p)$ with addition of $\omega_1(p)$. The last column gives the energy gradient based on distributed adiabatic plume convection of water of potential density sinking down to its level of neutral balance

Pressure (bar)	$\omega_0(p)$	$\omega_1(p)$	$\omega_2(p)$	$\omega_\phi(p)$	$\omega_T(p)$	$(\partial q / \partial p)_{\text{ad}}$ ($\text{J kg}^{-1} \text{ Pa}^{-1}$)
0	6785	5213	6222	0	5213	120
50	3094	2277	2369	32	2309	85
100	1403	1352	1428	21	1428	59
150	732	870	769	20	890	31
200	470	572	469	34	606	20
250	334	397	306	57	454	15
300	264	297	219	78	375	13
350	185	220	157	93	313	10
400	122	151	103	119	271	8
450	78	110	75	141	251	6
500	20	66	45	160	226	3
550	1	17	12	106	123	1

50 bar, however compensated by higher values at all levels deeper than 100 bar. From this it may seem that the notion of a nearly constant mass flux may not be entirely wrong for major parts of the depth range. It is, however, a fair indication that consistent with eq. (22) the vertical diffusivity varies considerably throughout the water column, values in the lower levels being roughly one order of magnitude greater than at near surface levels.

The computed values presented in Table 1 show that if the assumptions were valid, the required power supply for a constant vertical mass flux up through the water column is not very different from the available energies computed by eq. (24). The similarity is, however, not sufficient to support the notion of a constant vertical mass flux, such as being the consequence of adiabatic convection to the deepest bottom only. That will be evident from the computations presented in the following sections.

4.1.2. Adiabatic sinking of Norwegian Sea (NS) overflow water to the bottom of the North American Basin. More informative than the previous example of deep overturning circulation in the North Atlantic is an adiabatic convection scheme involving actual overflow water from the Denmark Strait, in this case with theoretical surface values $S = 34.918$ psu, $T_0 = -1.050$ °C (NSDW). The sinking down the continental slopes, eventually reaching the bottom water in the North American Basin, is assumed to be adiabatic with no detrainment and intrusion into the deep water of the North Atlantic except at the 550-bar level where assimilation takes place. The remaining part of the circulation is as already described.

The density of the sinking NSDW water is established by an iterative computation procedure based on the equation of Bryden (1973). The $p\Delta\alpha$ -cycle is shown in Fig. 5. From this, an astonishing high value of $q(p_B) = 35.87$ J kg⁻¹ is determined, more than twice that of the previous example. The main reason for this large difference lies in the very much lower specific volume of the assumed adiabatic descent of the NSDW ($T = -0.630$ °C as compared to $T = 2.059$ °C of the resident water at 550 bar). The corresponding flux rate of the ascending water masses is independent of depth and has a value of 1.38×10^9 kg s⁻¹.

A circulation like the one pictured above is totally unrealistic, not only because entrainment is ignored, contrary to observation, but also because adiabatic convection to the very bottom inevitably would influence the bottom water characteristics significantly. In reality, the pool of bottom water in the North American basin is overwhelmingly determined by inflow of water of Antarctic origin. That is clearly demonstrated by its salinity being lower than of both NSDW and NADW.

4.2. Convection and sinking to a range of (or all) depths in the system (scenario 2)

4.2.1. Adiabatic convection and sinking to a range of (or all) depths in the basin. This model assumes that convecting plumes from the surface reach down to and come to rest at virtually all levels in the basin (Fig. 6). It is also implied that the convecting

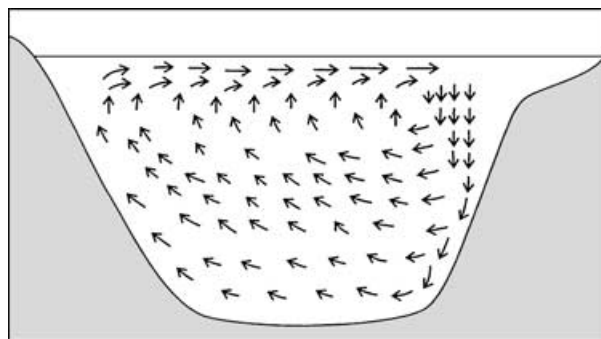


Fig 6. Schematic diagram of distributed adiabatic sinking of surface water with density identical to the potential density at the levels of intrusion.

water originates with a specific volume equal to the potential specific volume of the level where it comes to rest. This implies that no lateral mixing affects the falling plumes during the descent. Hence, there shall be no intrusion at other levels than that of equilibrium density. The corresponding circulation is the least energy requiring and should show maximum values of vertical mass fluxes in the upper part of the water column. The purpose of the exercise is to assess these maximum flux values. The bases for these computations are the power density values and the adiabatic energy density gradients $(\partial q / \partial p)_{ad}$, all listed in Table 1. Values of this gradient have been established by first determining individual $q(p)$ -values for a sufficiently dense set of $p\alpha$ -cycles, and the gradients are then derived from corresponding $\Delta q(p) / \Delta p$ ratios.

Table 2. North Atlantic vertical mass fluxes in 10^9 kg s⁻¹: $F_1(p)$, $F_2(p)$ and $F_3(p)$ based on distributed adiabatic plume convection of water of potential density to its level of neutral balance, $F_1(p)$ and $F_2(p)$ with diapycnal mixing only, $F_3(p)$ from $\omega_T(p)$ (with geothermal heat included). $F_4(p)$, $F_5(p)$ and $F_6(p)$ are based on descending NSDW and intruding at all levels, the two former with $\alpha = 1/2$ and $2/5$, $F_6(p)$ with $\alpha = 1/2$ and with potential energy from geothermal heat included

Pressure (bar)	$F_1(p)$	$F_2(p)$	$F_3(p)$	$F_4(p)$	$F_5(p)$	$F_6(p)$
0	4.34	5.18	4.76	2.29	2.74	2.30
50	2.68	2.79	2.72	2.06	2.15	2.09
100	2.38	2.29	2.42	2.79	2.68	2.83
150	2.82	2.48	2.87	4.09	3.62	4.19
200	2.86	2.35	3.03	3.66	3.00	3.88
250	2.65	2.04	3.03	2.65	2.04	3.03
300	2.28	1.68	2.88	2.10	1.55	2.66
350	2.20	1.57	3.13	1.71	1.22	2.43
400	1.89	1.29	3.39	1.36	0.93	2.45
450	1.83	1.25	4.19	1.14	0.77	2.59
500	2.20	1.50	7.53	0.8	0.55	2.76
550	1.70	1.20	12.30	0.2	0.15	1.61

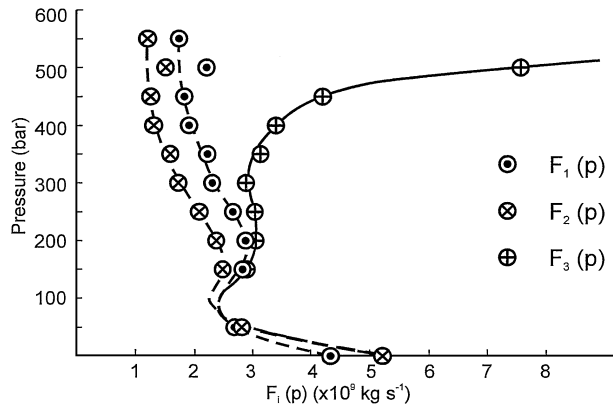


Fig 7. Upward total (advective and diffusive) mass fluxes $F_i(p)$ ($i = 1, 2, 3$) in 10^9 kg s^{-1} versus pressure, all related to distributed adiabatic convection and sinking of water to all levels in the basin, each branch with surface potential density as of the level of intrusion. Indices 1 and 3 refer to computed available power densities $\omega_1(p)$ and $\omega_T(p)$ as of Table 1. Index 2 same as 1, but with α in eq. (22) as $2/5$.

The computed mass fluxes $F_1(p)$ (Table 2, also shown in Fig. 7) are within the expected range and clearly far from being constant. Apart from conspicuously low values in the 50–150 bar range, $F_1(p)$ varies fairly systematically from a ‘bottom’ value of about $1.7 \times 10^9 \text{ kg s}^{-1}$ up to a ‘surface’ value of $4.34 \times 10^9 \text{ kg s}^{-1}$, a behavior consistent with a higher power input in the higher range of the water column. The tendency to growing values upward is an indication of formation of NADW and, above that, contribution from Mediterranean Water and North Atlantic Central Water (NACW), the latter strongly influenced by Ekman convergence in the subtropical gyre. The relatively low values of the upward mass fluxes seen in the 50–150 bar range may be a consequence of flow into the South Atlantic. The surface value of $4.34 \times 10^9 \text{ kg s}^{-1}$ may not seem as high as one would have expected in comparison with the result from the constant adiabatic flux case of $3.20 \times 10^9 \text{ kg s}^{-1}$. It should be kept in mind, however, that the higher mass fluxes of the upper levels are disproportionately more energy consuming because of the stronger density gradients in this part of the water column. It should also be noted that our procedure for evaluating gradients for the adiabatic case of plume convection is based on an assumption that the adiabatic lapse rate is a function of pressure only, which is an approximation with a minor systematic error.

Although the contribution to generation of potential energy from geothermal heat conversion ($\omega_\phi(p)$) is less than 10% of the total, the estimated values below the 300-bar level are considerable, and below the 400-bar level overwhelming in comparison with power toward diapycnal mixing. This is also reflected in the mass flux values $F_3(p)$ (Table 2, Fig. 7), which in the lower range are increasing with depth, in conflict with continuity requirement in a single basin. This indicates that the geothermal influence at these levels may be overrated, a matter further discussed in Section 5.6.

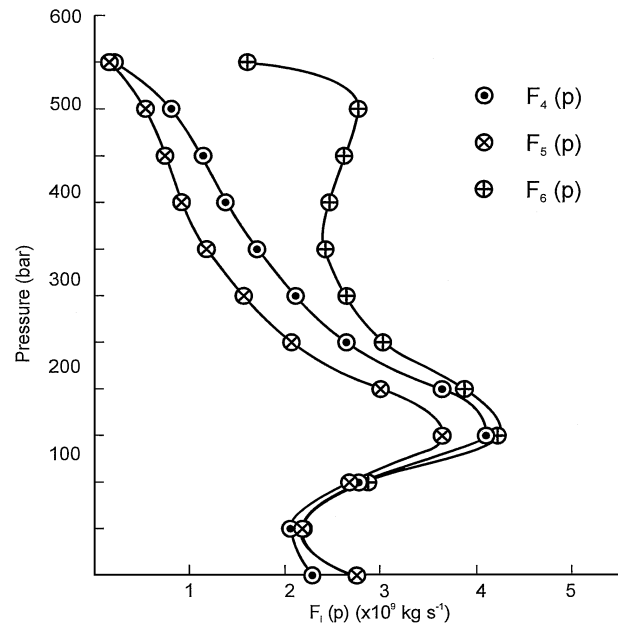


Fig 8. Upward total mass fluxes $F_i(p)$ ($i = 4, 5, 6$) in 10^9 kg s^{-1} versus pressure, all related to sinking and distributed intrusion of NSDW at all levels. Indices 4 and 6 refer to power densities $\omega_1(p)$ and $\omega_T(p)$, the latter with inclusion of geothermally generated potential energy, as of Table 1. Index 5 refers to values determined as with index 4, but with α in eq. (22) as $2/5$.

4.2.2. Non-adiabatic sinking to a range of (or all) depths in the basin. The last two columns of Table 2, $F_4(p)$ and $F_6(p)$, are the results of mass flux computations with isobaric intrusion and mixing of water from the descending bottom current east and south of Greenland. Most of this water is of NSDW origin, but it may also contain fractions of winter water from the Labrador Sea. The specific volume of the intruding water is as observed in the bottom current. The computations have been obtained from eq. (19) with power densities as in Table 1 and energy gradients directly from $\Delta\alpha$ based on actual specific volumes. Values below the 350-bar level have been obtained by extrapolation on assumption of an adiabatic lapse rate toward the bottom. These mass fluxes are also illustrated in Fig. 8.

As expected, the computed mass fluxes are generally above $1.38 \times 10^9 \text{ kg s}^{-1}$, which corresponds to adiabatic sinking to the 550-bar level only. Only in the deeper ranges toward the bottom lesser flux values are seen. The implication of the latter observation is that most of the sinking water has intruded at levels above 350 bar. It was also to be expected that the flux values should show a steadily increasing tendency upward in the water column, possibly approaching a near constant level in the upper 100-bar range. Such behavior is not fully supported by the computed $F_4(p)$ fluxes. Conspicuously high values are seen in the data from the 150–200 bar levels, a fact related to lower $\Delta\alpha$ -values at these levels. We are inclined to attribute this observation to ‘leakage’ from the main water body in this range, most

likely reflecting significant deep-water flows toward the Southern Hemisphere. Inclusion of potential energy from geothermal conversion ($F_6(p)$) does not change the picture significantly except in the lower range where higher fluxes are listed. As in the case with $F_3(p)$ the extraordinary high values below the 350-bar level may be explained by the geothermal influence being overrated (as discussed in Section 5.6). We also acknowledge that the extrapolation scheme applied to the lower range of sinking water of NSDW origin may cause the corresponding $\Delta\alpha$ -values to be inflated.

5. Discussion and conclusions

5.1. Basin configuration

In order to better understand the energetics of a system, we have limited our study to 'single basin hemispheric circulation', which employs the idea that the upward motion of the main body of water in the system is along a representative path in the $p\alpha$ -space. The North Atlantic has been chosen as an example because of presence of pronounced deep convection in the form of bottom currents as well as open ocean plumes (Marshall and Schott 1999). As the emphasis of the paper is on the method rather than validity of the numerical results, we have felt confident in treating the North Atlantic as a separate basin in spite of the obvious errors involved. The most conspicuous of these errors is ignoring the substantial exchanges with the South Atlantic.

5.2. Patterns of circulation

Although other forms of convection may exist in the ocean, the most common type of free convection is usually recognized to originate at the surface, and we have assumed that to be the case in our examples. As has been well known and also concluded by a series of model studies (e.g. Weaver et al. 1993; Huang 1999; Scott et al. 2001), we have assumed the source water for the process to be advected from the tropics by surface currents. We recognize that this feature may be unique for the North Atlantic, and that application of the presented models to other oceans, or to the global oceans as a whole, will require a different approach. As typical of the South Atlantic, a major portion of the source water for deep-water formation in the Antarctic is not surface water from the tropics, but essentially deep water from the North Atlantic. The corresponding thermodynamic cycle would then be considerably smaller, and with a given power supply, the overturning mass flux substantially larger.

The convection and related organized sinking have been assumed to be parts of a system of closed circulation(s), either as a single cell reaching to the bottom or as a system of multiple cells situated within each other. In the latter case, all cells contribute to support a common rising flow up through the main water body of the ocean. In the upper depth range, the upward flow gradually converges into a surface current with a meridional

component toward higher latitudes. The simplicity of the single basin concept applied to the North Atlantic practically precludes any multiple cell structure otherwise possible.

Whereas several convection scenarios are investigated, the rising main water body has remained the same and been chosen to surface with a temperature of about 23 °C at the eastern edge of the subtropical gyre. This choice was made for practical reasons and does not imply any conviction that the warm NACW of the subtropical gyre is, or is not, part of the meridional circulation. Centrally in the gyre the warm water is sinking, but sliding out and rising along the periphery. However, the fact remains that some portion of the warm water is leaking out along the western edge in the form of the Florida Current and the Gulf Stream. Compensation in the North Atlantic may well contain colder and less salty deeper water gradually entraining the entire flow field outside the warm water lens, as in the Canary Current or elsewhere. With the absence of rising water within the warm water lens, the horizontal area of the 50-bar level is greatly overrated. This should imply overestimated mass flux values, but in fact the computations show the opposite. Clearly, other effects more than compensate for this condition. The impact of Mediterranean water and higher up, the pronounced thermocline, both contributing to increase the gradient of eq. (19), may have effects in that direction.

5.3. Comparison with classical approach employing the concept of turbulent diffusivity

The present $p\alpha$ -method, employing the principle of circulation in closed cells, and the classical approach, where the effect of turbulence is described in terms of an eddy diffusivity K_z , have much in common. Both methods aim to establish mechanical energy budgets of the system, the former by determination of the work against pressure and associated power requirement of closed circulations in the system, the latter by focusing on production of potential energy in the main body of rising water in the system. As shown in Appendix C, the two methods are complementary in the sense that the mentioned power requirement of the system derives from potential energy produced in the water column. A slight distinction between the methods lies in that the $p\alpha$ -method recognizes potential energy production in the sinking water (as in the rising), and that a substantial portion of the power requirement toward this end actually derives from kinetic energy of the sinking water itself. Both methods depend ultimately on knowledge of the power converted to turbulence and insight into the efficiency of the turbulence in producing work against gravity, as well as of energy losses by internal convective adjustments.

Another property of the $p\alpha$ -method is that it allows for incorporation of geothermal driving and double diffusion as energy sources contributing to the overturning circulation. To do so, knowledge of the vertical distribution of the corresponding energy flux densities is required, or this may have to be inferred

from assessment of the total rate of energy supply from these sources on the basis of appropriate hypotheses.

5.4. Importance of compressibility

The computations of energy output $q(p)$ and related quantities have all been carried out with the specific volumes $\alpha(p)$ and $\alpha'(p)$ derived from known or stipulated values of temperature, salinity and pressure. This means that the effect of compressibility already is inherent. A question of theoretical interest is whether compressibility is of significance or perhaps important for the outcome of the energy output. A simple way to find out is to make the computations with the specific volume at all depths replaced with the potential specific volume (with reference to a fixed pressure, as with $p = 0$). With compressibility ignored, the energy output of a given cycle operating between the surface and the 550-bar pressure level, and with temperature, salinity and pressure as observed in the subtropical North Atlantic, the total energy output was reduced from 15.48 to 11.33 J kg⁻¹. The difference in this case is 4.15 J kg⁻¹, or roughly 27%.

It should then be clear that the property that sea water is compressible implies that the power required to drive the circulation of the real ocean is notably higher than that of an incompressible system working within the same potential temperature range. In other words, the compressibility of the sea water does not enhance overturning thermohaline circulation of the oceans involving the same water masses. It is, however, recognized that even a slight reduction of compressibility may lead to a complete change of convection regimes in the deep ocean, most likely to higher bottom water salinity and temperature.

5.5. Influence of surface distribution of salinity

There is no doubt that the global distribution of surface salinity has an overwhelming influence on the regimes of present-day deep-reaching convection and sinking. This is particularly the case with respect to the localities where bottom water may be formed. The general idea is that the surface salinity controls the density at freezing conditions and that in many regions of low surface salinity the density may not become sufficiently high to sustain deep-reaching convection. This fact is usually misinterpreted in the way that low surface salinity at higher latitudes per se is affecting large-scale thermal convection in a negative way. That is far from the truth. In order to address the problem we have compared the circulation of the first example in Section 4 (adiabatic convection in the North Atlantic), having an energy output of 15.48 J kg⁻¹, with that of thermal convection in an isohaline ocean operating within the same temperature range. The outcome of the latter is 28.8 J kg⁻¹, which is about 86% more than the former. Correspondingly higher power input would be necessary to drive a circulation of equal strength. Another computation with convection temperatures as observed resulted in an increase in the power requirement of 66%. Both examples in-

dicate that low surface salinity in waters where convection takes place is actually enhancing the overturning circulation significantly. The physical explanation behind this perhaps controversial statement is that with lower salinity the density of the heaviest possible bottom water is reduced. In consequence vertical diffusion is enhanced and likewise the corresponding velocity of ascent. Conclusions toward a similar effect were also reached by Nilsson and Walin (2001). Parametrizing diapycnal mixing using a constant energy concept (also discussed by Huang 1999) they found a steady-state solution for thermohaline circulation where freshwater forcing enhances the circulation. It may well be justified to assume that the discussed effect is roughly proportional to the meridional gradient of salinity, in which case a gradient increase of 0.1 psu should require about 2.8% less energy in order that the circulation rate should remain the same. This is an astonishing amount.

Before closing the topic, a final word about the comparison may be appropriate. Given the same rate of energy conversion in the sea, the isohaline circulation will clearly be slower than compared with the present. This means that the penetration of heat from above is likely to become stronger and to some extent reduce the density of the deep/bottom water and thereby weaken the predicated effect.

5.6. Role of geothermal heating

The role of geothermal heating has been assessed on the basis of heat flux data given by Stein and Stein (1992). These data are not specified directly as related to the depth, but to the age of the sediments at the ocean bottom, and a statistical relationship between the sediment age and the depth is shown in a scatter diagram. For our purpose the material has furthermore the weakness that very few data exist for depths less than 3000 m, and these observations appear to be widely scattered. However, these conditions may not be very important because our computations confirm that the relative role of geothermal heating in shallower regions is negligible.

Relative to the total generation rate of potential energy in the North Atlantic, the geothermal heat flux contributes with about 10%. Although seemingly a small fraction, the relative importance in the deeper ranges is quite different. Here geothermal heating seems to have an overwhelming influence. However, the calculated flux rates violate continuity conditions, an indication that the potential energy production at these levels is significantly overrated. Nevertheless, geothermal heating seems to be of consequence for the overall meridional overturning circulation, a conclusion in agreement with results of an idealized modeling experiment (Scott et al. 2001). The relative importance of geothermal heating is above all determined by the real value of R_f , or γ , of which there is some uncertainty. With $R_f = 0.05$, the relative contribution of geothermal heating to the overall generation of potential energy would increase from 10% to about 30% of the total.

In the presentation of generation of potential energy by geothermal heating it has been assumed that all generated potential energy is available to support overturning circulation in the ocean, meridional or not. This assumption may be far from the reality. Lateral differential heating will be a salient feature of the process, and internal convective adjustments of the stratification permanent processes along ridges and continental slopes. Associated dissipation and upward fluxes of heat are inevitable. The same is also true of potential energy generated by diapycnal mixing, but in that case the net effect may be incorporated in the semi-empirical efficiency γ . Corresponding ‘efficiency’ factors of the geothermal heat transfer are not known, and would in any case be strongly dependent on the topographic features of the ocean basin.

5.7. Conclusions

The main objectives of this paper have been to explore the possibility of investigating overturning circulation in the ocean by means of closed cycles in the $p\alpha$ -space, and in particular to recognize advantages and limitations of the method. Some of these are evident from the applications presented in the preceding section, in particular the simplicity by which the energy requirement of a given cycle may be determined. Others have been discussed in the subsections of this section. At present, the method should be regarded as equivalent and/or complementary to classical K_z -applications, in the future as likely an independent instrument toward assessment of overturning circulation in nature. In spite of the simplifications introduced, we feel that the study so far has been rewarding. A next step will be to find ways to apply the method to a real ocean with two or more main sources of deep-water formation.

6. Acknowledgment

The authors are indebted to Dr Knut Barthel for stimulating criticism and inspiring discussions.

7. Appendix A: on one-dimensional stationary vertical diffusion and advection balance

The production (rate) of potential energy ϕ per unit area by vertical diffusion is given by the sum of vertical eddy fluxes of mass up through the water column:

$$\phi = -g \int_{-D}^0 K_z(z) \frac{\partial \rho'}{\partial z} dz. \quad (\text{A1})$$

The gradient appearing in eq. (A1) is based on potential values of density with reference to level z . Simultaneously the vertical advective mass flux (density) $R(z)$ is

$$R(z) = w(z)\rho(z) \quad (\text{A2})$$

where $w(z)$ and $\rho(z)$ are *in situ* values. Stationary conditions require that

$$w(z)\rho(z) - K_z(z) \frac{\partial \rho'}{\partial z} = C. \quad (\text{A3})$$

At some lower level ($-D$) the gradient $\partial \rho' / \partial z$ is assumed to vanish. It follows that $C = w(-D)\rho(-D)$. As a consequence

$$w(z)\rho(z) - K_z \frac{\partial \rho'}{\partial z} = w(-D)\rho(-D). \quad (\text{A4})$$

Substitution of the diffusion term from this equation into eq. (A1) now leads to

$$\phi = g \int_{-D}^0 [w_{-D}\rho_{-D} - w(z)\rho(z)] dz. \quad (\text{A5})$$

An alternative expression is

$$\phi = w_{-D}\rho_{-D}g \int_{-D}^0 [w_{-D}\rho_{-D} - w(z)\rho(z)] \frac{dz}{w_{-D}\rho_{-D}}. \quad (\text{A6})$$

Because $w_{-D}\rho_{-D}$ is the constant mass flux up through the column, the following expression

$$I = g \int_{-D}^0 \frac{w_{-D}\rho_{-D} - w(z)\rho(z)}{w_{-D}\rho_{-D}} dz \quad (\text{A7})$$

is the work produced per unit mass as the particle moves from level $-D$ to the surface.

Let $\rho_{-D}^*(z)$ be the potential density of the bottom water at level z and let $w^*(z)$ be the corresponding velocity of an isolated particle moving up through the field. Now, if pressure were the only condition affecting the volume of the particle as it moves up through the water column, then the velocity $w^*(z)$ at any level must be identical to $w(z)$ and satisfy the condition

$$w^*(z)\rho_{-D}^*(z) = w_{-D}\rho_{-D}. \quad (\text{A8})$$

This allows us to substitute $w^*(z)\rho_{-D}^*(z)$ in both numerator and denominator of eq. (A7):

$$I = g \int_{-D}^0 \frac{w^*(z)\rho_{-D}^*(z) - w(z)\rho(z)}{w^*(z)\rho_{-D}^*(z)} dz. \quad (\text{A9})$$

Because the velocities appearing in eq. (A9) are identical, we may write the more simple form

$$I = g \int_{-D}^0 \frac{\rho_{-D}^*(z) - \rho(z)}{\rho_{-D}^*(z)} dz \quad (\text{A10})$$

as an equivalent expression for the work performed by the diffusion during the time it takes to move the particle from the bottom to the surface. As stated, if pressure were the only condition affecting the volume flux of the flow, the expression above is exact. With the non-linear influence of salinity and temperature on density taken into account, eq. (A10) will give a slightly reduced value, although in most cases adequate as an approximate measure of the work involved.

8. Appendix B: generation of potential energy by geothermal heat transfer

Let \dot{Q} be the heat flux density through the horizontal projection of the bottom; α is the thermal expansion coefficient at constant pressure and c_p the specific heat capacity of the bottom water at that pressure. $\rho(z)$ is the *in situ* density up through the water column. Observations from water masses at great depths indicate generally a stable stratification down to the lowermost few hundred meters. We are therefore justified in assuming that in the initial stage a weak warming of a bottom layer of thickness h will take place. By thermal expansion the bottom layer will grow in thickness according to

$$\frac{dh}{dt} = \frac{\alpha \dot{Q}}{\rho' c_p} \quad (\text{B1})$$

where ρ' is the density of the bottom layer. The expansion process of eq. (B1) causes a general uplift of the entire water column. The corresponding rate of change of potential energy follows from differentiation of the potential energy PE , here measured relative to any arbitrary level $-H$ situated below the bottom at $-D$:

$$\frac{d}{dt} \frac{PE}{g} = M \frac{dH}{dt} + \frac{d}{dt} \int_{-D}^{-\zeta} \rho' z dz + \frac{d}{dt} \int_{-\zeta}^0 \rho(z) z dz. \quad (\text{B2})$$

M is the total mass per unit surface of the entire water column and $-\zeta$ is the level of the upper limitation of the homogeneous bottom layer, so that $h = -\zeta - (-D)$. Further development of eq. (B2) now leads to the simple expression

$$\phi = \frac{dPE}{dt} = g \left(M - \frac{m}{2} \right) \frac{dh}{dt}. \quad (\text{B3})$$

Here m is the mass per unit cross-section of the bottom layer. By substitution of the lhs of eq. (B1) the rate of generation of potential energy becomes

$$\phi = g \left(M - \frac{m}{2} \right) \frac{\alpha \dot{Q}}{\rho' c_p} \approx g \bar{\rho} D \frac{\alpha \dot{Q}}{\rho' c_p}. \quad (\text{B4})$$

The latter expression is the same as in eq. (2).

9. Appendix C: equivalence of the $p\alpha$ -cycle

The following development is based on the assumptions that the pressure field everywhere is hydrostatic, that deep return flow takes place along a geopotential level surface, and that this also is isobaric. The depth of this geopotential surface measured from the free surface is D at the location of sinking, while being $D + \delta$ at the location of rising. This is clearly an approximation because the water is in motion, but considering the extremely small velocities involved, the error is probably negligible. The integral of eq. (6) is then conveniently expressed in terms of pressure as independent variable ($p = p(z)$):

$$J = \oint p d\alpha = \int_0^{p[-(D+\delta)]} \alpha dp - \int_0^{p(-D)} \alpha' dp. \quad (\text{C1})$$

The integrations are preferably carried out with the vertical coordinate z substituting the pressure

$$J = g \int_{-(D+\delta)}^0 \alpha \rho dz - g \int_{-D}^0 \alpha' \rho' dz. \quad (\text{C2})$$

It follows from this that the whole expression reduces to

$$J = g(D + \delta - D) = g\delta. \quad (\text{C3})$$

In order to interpret this form we observe that

$$\int_{-(D+\delta)}^0 \rho dz = \int_{-D}^0 \rho dz + \rho_{-D} \delta = \int_{-D}^0 \rho' dz. \quad (\text{C4})$$

From this equation δ is sought and substituted into eq. (C3) from which it follows that

$$J = g\delta = \frac{g}{\rho_{-D}} \int_{-D}^0 (\rho' - \rho) dz \quad (\text{C5})$$

where ρ_{-D} is the low-level density of the rising water at path (1). Finally we split the integral into two separate terms by adding and subtracting a constant ρ_{-D} :

$$J = g \int_{-D}^0 \frac{\rho_{-D} - \rho(z)}{\rho_{-D}} dz + g \int_{-D}^0 \frac{\rho'(z) - \rho_{-D}}{\rho_{-D}} dz. \quad (\text{C6})$$

This form is the same as eq. (7).

References

- Arneborg, L. 2002. Mixing efficiencies in patchy turbulence. *J. Phys. Oceanogr.* **32**, 1496–1506.
- Bjerknes, V. 1898. Über einen hydrodynamischen Fundamentalsatz und seine Anwendung bes. auf die Mechanik der Atmosphäre und des Weltmeeres. *Kungliga Svenska Vetenskapsliga Akademiens Handlingar*, **31**, 1–35 (in German).
- Bryden, H. L. 1973. New polynomials for thermal expansion, adiabatic temperature and potential temperature of sea water. *Deep-Sea Res.* **20**, 401–408.
- Colin de Verdière, A. 1993. On the oceanic thermohaline circulation. In: *Modelling Oceanic Climate Interactions*, (eds J. Willebrand and D. L. T. Anderson). Springer-Verlag, Berlin, 151–184.
- Defant, A. 1961. *Physical Oceanography I*. Pergamon Press, Oxford, 729 pp.
- Fjeldstad, J. E. 1936. Results of tidal observations. Norwegian North Polar Exped. with the Maud 1918–1925. *Scientific Results* **4**, 88 pp.
- Egbert, G. D. and Ray, R. D. 2000. Significant dissipation of tidal energy in the deep ocean inferred from satellite altimeter data. *Nature* **405**, 775–778.
- Egbert, G. D. and Ray, R. D. 2001. Estimates of M2 tidal energy global dissipation from TOPEX/Poseidon altimeter data. *J. Geophys. Res.* **106**, 22 457–22 502.
- Gade, H. G. 1968. Horizontal and vertical exchanges and diffusion in the water masses of the Oslo Fjord. *Helgoländer wissenschaftliche Meeresuntersuchungen* **17**, 462–475.
- Gade, H. G. and Edwards, A. 1980. Deep water renewal in fjords. In: *Fjord Oceanography*, (eds H. J. Freeland and D. M. Farmer). Plenum, New York, 453–489.

- Gargett, A. E. 1984. Vertical eddy diffusivity in the ocean interior. *J. Mar. Res.* **42**, 359–393.
- Gargett, A. E. and Holloway, G. 1984. Dissipation and diffusion by internal wave breaking. *J. Mar. Res.* **42**, 15–27.
- Godske, C. L., Bergeron, T., Bjerknes, J. and Bundgaard, R. C. 1957. *Dynamic Meteorology and Weather Forecasting* Am. Meteorol. Soc., 800 pp.
- Göransson, C.-G. and Svensson, T. 1975. *Byfjorden: Vattenomsättning*. Statens Naturvårdsverk, Stockholm, 152 pp. (in Swedish).
- Gustafsson, K. E. 2001. Computations of the energy flux to mixing processes via baroclinic wave drag on barotropic tides. *Deep-Sea Res. I* **48**, 2283–2295.
- Huang, R. X. 1999. Mixing and energetics of the oceanic thermohaline circulation. *J. Phys. Oceanogr.* **29**, 727–746.
- Jeffreys, H. 1925. On fluid motions produced by differences of temperature and humidity. *Q. J. R. Meteorol. Soc.* **51**, 347–356.
- Levitus, S. and Boyer, T. P. 1994. *World Ocean Atlas 1994, Vol. 4, Temperature*, NOAA Atlas NESDIS 4. US Department of Commerce, Washington, DC.
- Levitus, S., Burgett, R. and Boyer, T. P. 1994. *World Ocean Atlas 1994, Vol. 3, Salinity*, NOAA Atlas NESDIS 3. US Department of Commerce, Washington, DC.
- Marshall, J. and Schott, F. 1999. Open-ocean convection: Observations, theory, and models. *Rev. Geophys.* **37**, 1–64.
- Munk, W. 1966. Abyssal recipes. *Deep-Sea Res.* **13**, 707–730.
- Munk, W. and Wunsch, C. 1998. Abyssal recipes II: energetics of tidal and wind mixing. *Deep-Sea Res. I* **45**, 997–2010.
- Nilsson, J. and Walin, G. 2001. Freshwater forcing as a booster of thermohaline circulation. *Tellus A* **53**, 629–641.
- Osborn, T. R. 1980. Estimates of the local rate of diffusion from dissipation measurements. *J. Phys. Oceanogr.* **10**, 83–89.
- Pedersen, Fl. B. 1980. A monograph on turbulent entrainment and friction in two-layer stratified flow. *Series Paper No. 25*. Inst. of Hydrodynamics and Hydraulic Engineering, Tech. Univ. of Denmark, 397 pp.
- Proudman, J. 1953. *Dynamical Oceanography*. Methuen, London, 409 pp.
- Sandström, J. W. 1908. Dynamische Versuche mit Meerwasser. *Annalen der Hydrographie und Maritimen Meteorologie*, 6–23 (in German).
- Sandström, J. W. 1916. Meteorologische Studien in Schwedischen Hochgebirge. *Göteborgs Kungliga Vetenskaps- og Vitterhetssamhällets Handlingar*. 48 pp (in German).
- Scott, J. R., Marotzke, J. and Adcroft, A. 2001. Geothermal heating and its influence on the meridional overturning circulation. *J. Geophys. Res.* **106**, 31 141–31 154.
- Sjöberg, B. and Stigebrandt, A. 1992. Computations of the geographical distribution of the energy flux to mixing processes via internal tides and the associated vertical circulation in the ocean. *Deep-Sea Res.* **39**, 269–291.
- Stein, C. A. and Stein, S. 1992. A model for the global variation in oceanic depth and heat flow with lithospheric age. *Nature* **359**, 123–129.
- Stigebrandt, A. 1976. Vertical diffusion driven by internal waves in a sill fjord. *J. Phys. Oceanogr.* **6**, 486–495.
- Stigebrandt, A. 1979. Observational evidence for vertical diffusion driven by internal waves of tidal origin in the Oslofjord. *J. Phys. Oceanogr.* **9**, 435–441.
- Stigebrandt, A. and Aure, J. 1989. On vertical mixing in the basin waters of fjords. *J. Phys. Oceanogr.* **19**, 917–926.
- Taylor, G. I. 1931. Internal waves and turbulence in a fluid of variable density. *Rapp. et Proc. -verb. Reun. Cons. int. Explor. Mer.* **76**, 35–43.
- Weaver, A. J., Marotzke, J., Cummins, P. F. and Sarachik, E. S. 1993. Stability and variability of the thermohaline circulation. *J. Phys. Oceanogr.* **23**, 39–60.
- Welander, P. 1968. Theoretical forms for the vertical exchange coefficient in a stratified fluid with application to lakes and seas. *ACTA, RSSL Gothoburgensis, Geophysica* **1**, 3–26.
- Wunsch, C. 1998. The work done by the wind on the oceanic general circulation. *J. Phys. Oceanogr.* **28**, 2332–2340.
- Wunsch, C. and Ferrari, R. 2004. Vertical mixing, energy, and the general circulation of the oceans. *Ann. Rev. Fluid Mech.* **36**, 281–314.